A fully automated microfluidic-based electrochemical sensor for real-time bacteria detection

Zeynep Altintas, Mete Akgun, Guzin Kokturk, Yildiz Uludag

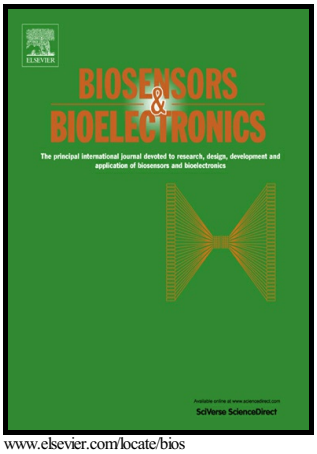

www.elsevier.com/locate/bios

PII: S0956-5663(17)30654-1
DOI: https://doi.org/10.1016/j.bios.2017.09.046
Reference: BIOS10020

To appear in: *Biosensors and Bioelectronic*

Received date: 25 July 2017
Revised date: 19 September 2017
Accepted date: 26 September 2017

Cite this article as: Zeynep Altintas, Mete Akgun, Guzin Kokturk and Yildiz Uludag, A fully automated microfluidic-based electrochemical sensor for real-time bacteria detection, *Biosensors and Bioelectronic,* https://doi.org/10.1016/j.bios.2017.09.046

A fully automated microfluidic-based electrochemical sensor for real-time bacteria detection

Zeynep Altintas[1]*, Mete Akgun[2], Guzin Kokturk[2], Yildiz Uludag[2]

[1]Technical University of Berlin, Straße des 17. Juni 124, Berlin, 10623 Germany

[2]UEKAE - BILGEM - The Scientific and Technological Research Council of Turkey (TUBITAK), Kocaeli, 41470 Turkey

*Corresponding author

Z. Altintas

Tel: +49 30 314 23727

Fax: +49 30 314 79552

e-mail: zeynep.altintas@tu-berlin.de

Abstract

A fully automated microfluidic-based electrochemical biosensor was designed and manufactured for pathogen detection. The quantification of *Escherichia coli* was investigated with standard and nanomaterial amplified immunoassays in the concentration ranges of 1.99×10^{4}–3.98×10^{9} cfu mL^{-1} and 10–$3.97x10^{7}$ cfu mL^{-1} which resulted in detection limits of 1.99×10^{4} cfu mL^{-1} and 50 cfu mL^{-1}, respectively. The developed methodology was then applied for *E. coli* quantification in water samples using nanomaterial modified assay. Same detection limit for *E. coli* was achieved for real sample analysis with a little decrease on the sensor signal. Cross-reactivity studies were conducted by testing *Shigella*, *Salmonella* spp., *Salmonella typhimurium* and *Staphylococcus aureus* on *E. coli* specific antibody surface that confirmed the high specificity of the developed immunoassays. The sensor surface could be regenerated multiple times which significantly reduces the cost of the system. Our custom-designed biosensor is capable of detecting bacteria with high sensitivity and specificity, and can serve as a promising tool for pathogen detection.

Keywords: Real-time pathogen detection, *Escherichia coli*, Microfluidic-based electrochemical sensor, Amperometry, Waterborne diseases.

1. Introduction

Bacteria related waterborne diseases are one of the major health problems in the world. Enormous effort is put into the development of modern technologies to obtain safe drinking water (Borgohain and Baruah 2017). Contamination of water sources with bacteria is a big problem not only in the developing but also in the developed countries (Florentin et al. 2016; Hancock et al. 1998; Lemarchand and Lebaron 2003). The majority of individuals who are affected by waterborne pathogens are infants, children, immunocompromised and elderly people.

Escherichia coli strains are facultative anaerobic members of Enterobacteriaceae family that normally found in the human intestinal flora in vast numbers and generally do not lead to any harm. However, their presence in the other parts of the body can cause serious diseases including diarrhea, meningitis, anemia, urinary tract infections and kidney failure. Enteropathogenic strains of *E. coli* can be classified based on their virulence factors: enterohaemorrhagic *E. coli* (EHEC), enterotoxigenic *E. coli* (ETEC), enteropathogenic *E. coli* (EPEC), enteroinvasive *E.coli* (EIEC), enteroaggregative *E. coli* (EAEC) and diffusely adherent *E. coli* (DAEC). To date, all of these pathogens were detected in water sources and human beings are considered as the main reservoir for entropathogenic *E. coli* strains (EHEC, ETEC, EIEC) (Nataro and Kaper 1998). The current methods used for bacteria detection are cultivation techniques, polymerase chain reaction (PCR) and the combined methods of these two (Velusamy et al. 2010). As these techniques are quite time consuming and expensive there is a continuous interest to develop rapid and sensitive detection methods.

Biosensors can be considered as a cutting-edge technology since they offer remarkable advantages over the other methods for the detection of bacteria. Enormous improvements, particularly with the aid of smart nanomaterials, have increased the successful applications of this technology for pathogen detection in different matrices (Ahmed et al. 2014; Boehle et al. 2017; Chen et al. 2017; Lazcka et al. 2007; Rasooly and Herold 2006; Rasooly et al. 2007; Struss et al. 2010). Fast, real-time, sensitive and specific biodetection assays using various sensor platforms have been employed for pathogen detection to prevent from threatening diseases (Adkins et al. 2017; Golabi et al. 2017; Masdor et al. 2016; Vaisocherova-Lisalova et al. 2016). Electrochemical biosensors and microfluidic devices are among the best examples of biosensing platforms for the detection of pathogenic bacteria. An electrochemical biosensor for the detection of E. coli O157:H7 has recently been

developed with bi-functional glucose oxidase-polydopamine nanocomposites and Prussian blue modified screen-printed interdigitated electrodes (Xu et al. 2016). Label-free electrochemical detection of *E. coli* based on rolling circle amplifications coupled peroxidase-mimicking DNAzyme amplification has shown good potential for food safety analysis and clinical diagnosis (Guo et al. 2016). Microfludic based biosensors by embedding antimicrobial peptide-labelled beads could detect *E. coli* with a rapid and sensitive method (Yoo et al. 2014). Several other electrochemical and microfluidic-based biosensors have been reported for pathogenic bacteria detection by employing various nanomaterials in the sensing systems such as magnetic nanoparticles (Chan et al. 2013), carbon nanotubes (Zhang et al. 2016) and silver nanoparticles (Abbaspour et al. 2015). These biosensors display great potential for the detection of foodborne and waterborne bacteria with extremely high sensitivities.

In this study, a fully automated novel microfluidic-based electrochemical biosensor was designed and manufactured (**Scheme 1**A). The key features of MiSens device are the integrated microfluidic system, the new biochip design and real-time amperometric measurements. Integration of the microfluidics, the necessary electronic connections and electrode array is the major problem faced during the design and fabrication of the sensor device. Although a number of alternative strategies were reported in the literature for this purpose, these fabrication techniques are generally expensive, time consuming and labour intensive to be used for a commercially practicable device (Huang and Mason 2013; Yang et al. 2014). Our portable analyser device is composed of an electromechanical unit that controls the assay protocol through its integrated software (MiCont^{TM}). The sensor chip was developed for optimized surface chemistry and assay conditions for measuring HRP-TMB interaction as the measurement relies on the enzymatic reaction between these reagents. Immunoassays for pathogen quantification were then developed by targeting *E. coli*. For the first time, it was demonstrated that our custom designed fully automated biosensor device is capable of monitoring and detecting bacteria pathogens with the developed assay protocols.

A)

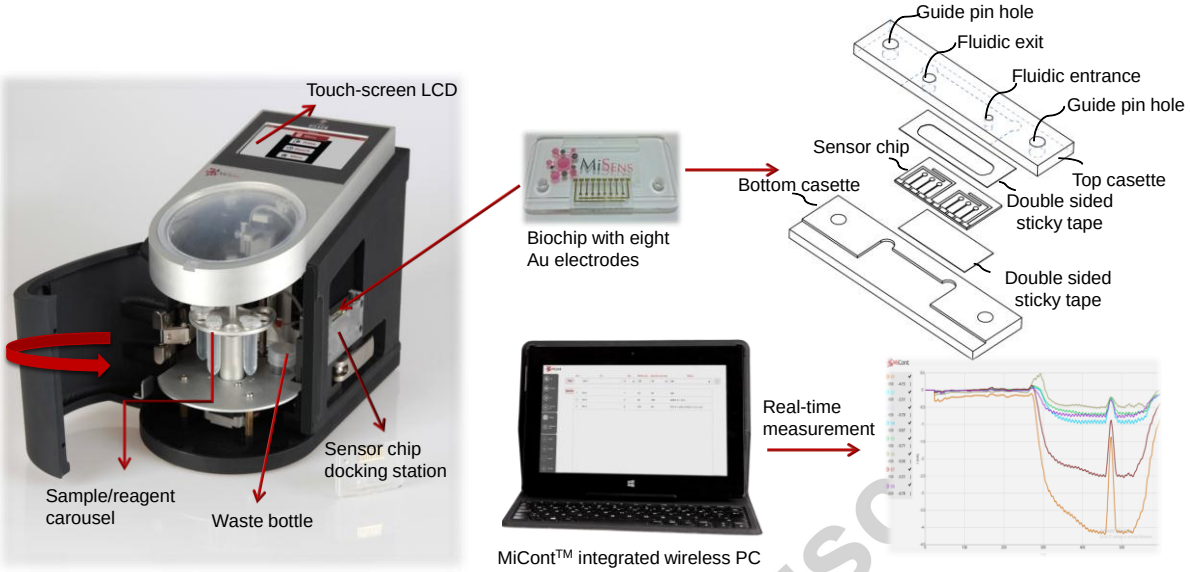

B)

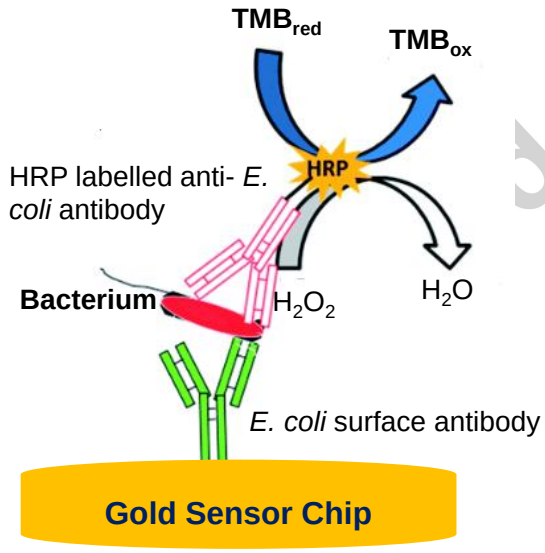

Scheme 1: A) Illustration of custom-designed MiSens biosensor. B) Pathogen detection assay.

2. Materials and Methods

2.1. Materials and reagents

A polyclonal rabbit anti- *E.coli* antibody (4329-4906) was purchased from BIO-RAD (Germany). *E. coli* samples were purchased from SeraCare Life Sciences (Gaithersburg, USA). *Salmonella, Shigella, S. aureus* and *S. typhimurium* were obtained from Public Health Agency (Ankara, Turkey). Phosphate-buffered saline tablets (PBS, 0.01 M phosphate buffer, 0.137 M sodium chloride and 0.0027 M potassium chloride, pH 7.4), mercaptoundecanoic acid (MUDA), mercaptoethanol, N-hydroxysuccinimide (NHS), ethanolamine, analytical grade ethanol, horse radish peroxidase (HRP), 3,3′,5,5′-tetramethylbenzidine (TMB) ready to use reagent (includes H_2O_2), were purchased from Sigma-Aldrich (Poole, UK). 1-Ethyl-3-(3-dimethylaminopropyl)-carbodiimide (EDC) was purchased from Thermo Scientific. Gold nanoparticles (40 nm) were obtained from BBI International (Cardiff, UK). Potassium chloride (KCl) was purchased from Fisher Scientific (Loughborough, UK). Ultrapure water (18 MΩ cm^{-1}) was obtained from a Milli-Q water system (Millipore Corp., Tokyo, Japan).

2.2. Instrumentation

Cyclic voltammetry and amperometric measurements were carried out using an integrated and fully automated electrochemical biosensor (MiSens) which was designed and fabricated in TUBITAK-BILGEM by our multi-disciplinary team (Scheme 1). MiSens device is controlled by using the developed MiCont^{TM} software (TUBİTAK-BİLGEM, Turkey) running on a wireless tablet. The sensor chip lay out was repressed on silicon dioxide wafer (Uludag et al. 2016a). The new design manufactured for this work consists of 8 sets of Au electrode arrays; each set possesses 3 working electrodes (d=1 mm) with shared Au counter and quasi-reference electrodes. Multiple Au electrodes set gives the opportunity to measure each sample with 8 electrodes simultaneously. This is also important to confirm the stability of the system and quality of the electrode production. Cyclic voltammetry (CV) tests were performed for electrode characterization using 1 mM potassium ferricyanide solution in 1M KCl with a scan rate of 0.1 V s^{-1} between -0.5 and 0.2 V. Amperometric measurements for the detection assays were conducted at -0.1 V.

2.3. Biochip surface modification

To obtain a clean sensor surface and successful surface modification, plasma cleaning was applied on the electrode arrays (Altintas et al. 2012b) and a self-assembled monolayer (SAM) was then formed by immersing the sensor chips in ethanolic solution of 2 mM MUDA (80 % or 100%) for overnight (Altintas et al. 2012b). The electrode arrays were then washed with ethanol and water prior to drying in fume hood. Later the arrays were packed with oxygen

barrier package and stored at +4ºC until use. SAM coated electrode arrays and the poly(methyl methacrylate) (PMMA) cassettes were combined using a double sided sticky tape (**Scheme 1**A). The sensor chip was then inserted into the sensor docking station to constitute the electronic and fluidic connections to form a microfluidic channel (~7 µl). Cyclic voltammetry measurements were applied with 1 mM potassium ferrocyanide solution in 1M KCl for surface characterization prior to antibody immobilization on the sensing areas via conventional amine coupling chemistry. Phosphate buffered saline (PBS, pH 7.4) was used as the running buffer and continuously flowed over the sensor surfaces between the injections. The sensor surfaces were initially activated with a 1:1 mixture of 0.4 M EDC and 0.1 M NHS and later a 200 µl anti- *E. coli* antibody in NaAc buffer (pH 4.5, 50 µl min^{-1}) were injected across sensor surfaces. Fourier-transform infrared spectroscopy (FT-IR) characterization of electrode surface before and after EDC-NHS activation were also performed. The detail information on FT-IR measurements is provided in Supplementary document. Non-reacted NHS esters were capped by injecting a 200 µl solution of 30 µg mL^{-1} of BSA (50 µl min^{-1}) and 1M of ethanolamine (pH 8.5, 50 µl min^{-1}), respectively.

2.4. Optimization of assay conditions and surface chemistry

The assay protocol requires an enzymatic reaction occurring in the presence of horse radish peroxides (HRP) and 3,3',5,5'-Tetramethylbenzidine (TMB) reagent as a substrate. Due to the importance of this reaction for the research outputs on MiSens biosensor, the binding event between HRP and TMB was initially investigated by utilizing incubation and also different surface chemistries. With this aim, one set of experiment was conducted with 4 min incubation of HRP with TMB reagent before injecting onto the sensor surface while the other set was performed without incubation. A 150 µL HRP-TMB solution was injected to the system with a flow rate of 50 µL min^{-1} and the real-time sensor signal was recorded at -0.1 V using amperometry method. PBS buffer (4 min, 100 µL min^{-1}) and HCI (1 min, 120 µL min^{-1}) were then injected into the system for cleaning the surface from HRP-TMB. Eight separate working electrodes of the chip were also evaluated to observe the variation between different electrodes and determine the stability of the sensor signal (**Fig. S1**). Furthermore, two different preparations (100 % and 80%) of 2 mM MUDA were tested to identify the best surface chemistry to form the self-assembled monolayer for the assays and the most convenient conditions were determined. The 80 % MUDA solution was prepared using a 2 mM mercaptoethanol (20%). The sensor signals with the different concentrations of HRP

were then compared and the optimum HRP concentration was selected to be used throughout the *E. coli* research.

2.5. *E. coli* detection assays

E. coli polyclonal antibody was used for antibody immobilization after CV characterization of the sensor chips. The concentration of antibody to be immobilized on the sensor surface generally ranging between 25 µg mL^{-1} and 50 µg mL^{-1} (Altintas et al. 2012a; Altintas et al. 2012b; Altintas et al. 2011). Due to this fact, antibody immobilization was optimized using two different concentrations (25 µg mL^{-1} and 50 µg mL^{-1}) of the surface antibody using the protocol given in Section 2.3. In this preliminary tests, a certain concentration of *E. coli* (3.5×10^6 cfu mL^{-1}) was used. The standard and nanomaterial amplified sandwich assays were then developed.

2.5.1. Standard sandwich assay

The sandwich immunoassay developed in this work has utilized polyclonal antibodies, which bound to different sites on the *E. coli* (**Scheme 1**B). The surface antibody, which is highly specific for the target, was attached to the sensor chip surface. The *E. coli* was then added, followed by addition of a HRP labelled secondary antibody referred to as the detection antibody. The detection antibody binds the *E. coli* at a different epitope than the surface antibody. As a result, the bacterium was 'sandwiched' between the two antibodies. The antibody binding affinity for the target is generally the main determinant of immunoassay sensitivity. Therefore, when the bacterium concentration increases, the amount of HRP labelled detection antibody increases, leading to a higher measured response in the presence of HRP substrate (TMB reagent).

For the assays, the self-assembled monolayer coated sensor chip was first docked to the instrument and primed with running buffer (PBS). Polyclonal rabbit anti- *E. coli* antibody was then immobilized onto the sensor surface via flow path of the instrument. The immobilization stage of the immunoassay was obtained using conventional amine coupling chemistry. *E. coli* samples in the concentration range of 1.99×10^4-3.98×10^9 cfu mL^{-1} were then prepared and each sample was injected to the antibody coated electrode surfaces for 8 min with a flow rate of 25 µL min^{-1} followed by the 8 min injection of HRP conjugated-detector antibody with same flow rate. Amperometric measurement was then performed at -0.1 V during a 4 min injection of TMB reagent (50 µL min^{-1}) followed by another 4 min for

buffer injection (100 µL min^{-1}). The surface was regenerated using 0.1 M HCI (1 min, 120 µL min^{-1}) for the detection of various concentrations of *E. coli*.

2.5.2. Nanomaterial amplified sandwich assay

The antibodies can be adsorbed on the AuNP surface at their isoelectric point by means of electrostatic interactions (Pawula et al. 2016; Uludag et al. 2016b). The same approach was applied in this study to enhance the detection capacity of the sensor for *E. coli* quantification. Briefly, a 1000 µL of AuNP solution was added to a 1.5 mL Eppendorf tube and a 5 µL of NaOH (0.2 M) was then added and mixed well. A 2.5 µL HRP in water (1 mg mL^{-1}) and 1.5 µL detection antibody were mixed and then added to AuNP solution. The tube was covered with an aluminium foil to avoid from light and rotated on a shaker at 600 rpm during 45 minutes. The solution was then centrifuged at 8000 rpm for 30 minutes at 4^{o}C and the supernatant was removed from the tube afterwards prior to addition of 33 µL BSA (10 mg mL^{-1}) and 70 µL PBS buffer (10 mM), respectively. The concentration of nanoparticles was calculated using a spectrophotometer at 525 nm wavelength and the AuNP solution was diluted based on the dilution factor calculated by considering the OD value. Since the dilution factor can show a batch-to-batch variation, AuNP assays were conducted using two different batches of the conjugated AuNPs and the results were compared. The detection of *E. coli* in the concentration range of 10-3.97×10^{7} cfu mL^{-1} was then investigated after immobilizing primary *E. coli* antibody onto electrode surfaces using 50 µg mL^{-1} antibody concentration (in NaAc buffer, pH: 4.5). The detection assays with AuNP-functionalized HRP conjugated detector antibody were performed using the same protocol given for standard sandwich assays.

2.6. Cross-reactivity studies

To check the specificity of the developed assays for *E. coli*, the binding of non-specific bacteria on *E. coli* antibody immobilized surfaces were investigated. A 10^{4} cfu mL^{-1} concentration of *Shigella*, *Salmonella* spp., *Salmonella typhimurium* and *Staphylococcus aureus* was injected onto the sensor (200 µl, 25 µl min^{-1}) and the binding results were evaluated in addition to the specific binding of 10^{4} cfu mL^{-1} *E. coli*. The sensor response of non-specific interactions was then calculated and expressed as percentage (%).

3. Results and Discussions

In our earlier studies, an electrode array was developed that utilizes shared reference and counter electrodes to minimize the size of the sensor. The selected dimension of the electrode size also enabled us avoiding photolithography and resulted in a cheaper and simpler way of producing sensor chips (Ciftci et al. 2016; Olcer et al. 2014). A new plug and play type biochip docking station was then designed that forms a flow cell (~7 μL) on the electrode array together with the electronic and microfluidic connections. The mechanical components of the MiSens device include a pump, biochip docking station, microfluidic tubing connected sample pick up needle, sample/reagent carousel and a waste bottle. The electronic parts of the device contain a multiplexed potentiostat, an LCD display, a digital control circuit and wired/wireless communication interface. The experiments can be conducted by using the MiCont^{TM} software running on a wireless PC/tablet. The protocols of the assays generated by the user can be saved and reused when required (**Scheme 1**A).

3.1. Optimization of assay conditions and surface chemistry development

Incubated HRP-TMB samples provided ~5 times higher signal than those of non-incubated samples as it is demonstrated in **Fig. 1**A. These assays were repeated three times on each individual electrode and the results also confirmed that signal variation was quite acceptable between separate electrodes. The used HRP concentration for the assays was 12.5 ng mL^{-1}. As being a moderate concentration, 12.5 ng mL^{-1} was a good choice for an optimization study, since it is possible to see a drastic decrease on the sensor response in the case of higher concentrations due to the saturation effect. On the other hand, much lower concentration might be lack of producing sufficient signal. The sensor chips employed for this comparative investigation was coated with 100% mercaptoundecanoic acid (2 mM MUDA) to obtain a self-assembled monolayer (SAM) prior to conduct HRP-TMB assays. After the confirmation of necessity of sample incubation prior to taking measurement, surface chemistry development was also investigated using two different coating solutions: 100% MUDA and 80% MUDA. We have chosen these concentrations based on our previous works (Altintas et al. 2011; Uludag et al. 2016a). One set of sensor chips was immersed in 100% MUDA and the other set was immersed in 80% MUDA. The incubated HRP-TMB samples (12.5 ng mL^{-1}) were then separately analysed on these sensor chips. It was clearly observed that the surfaces coated with 100% MUDA produced more stable and reliable results with minimal standard errors when compared to 80% MUDA coated sensor chips (**Fig. 1**B).

A)

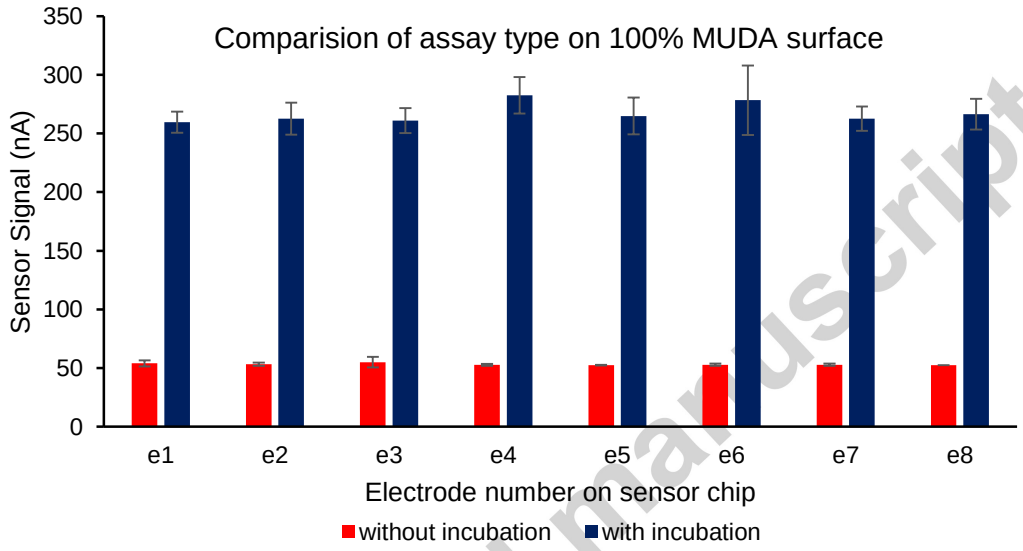

B)

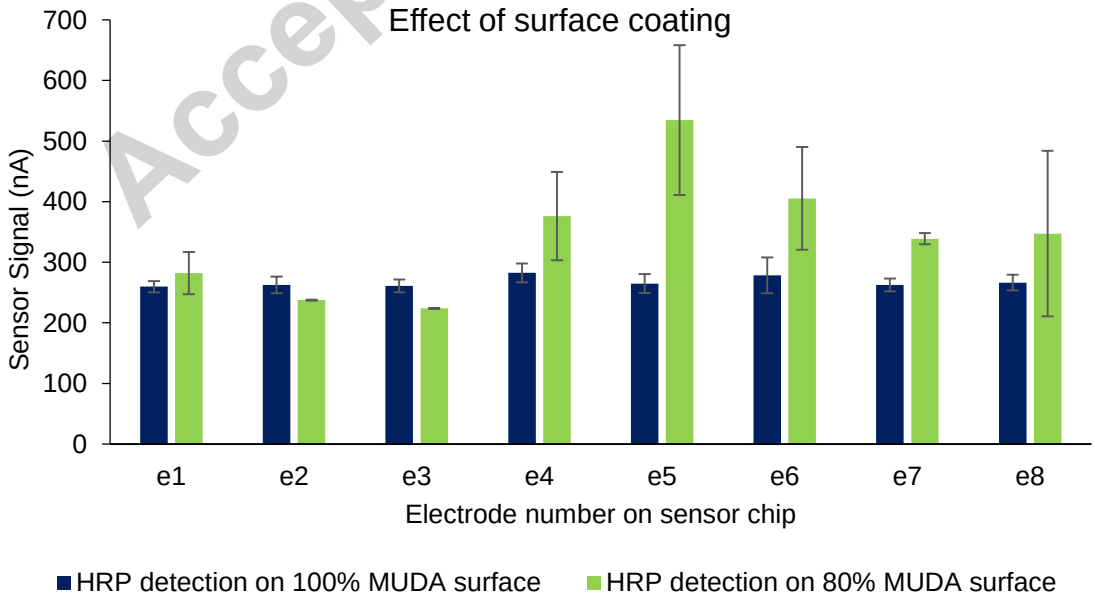

C)

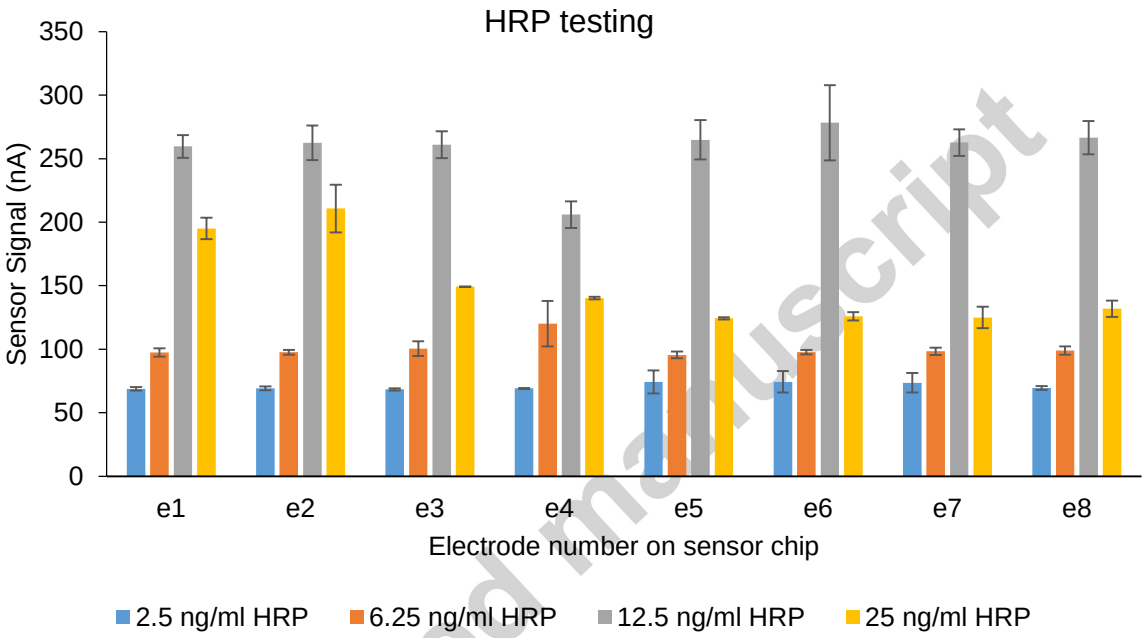

D)

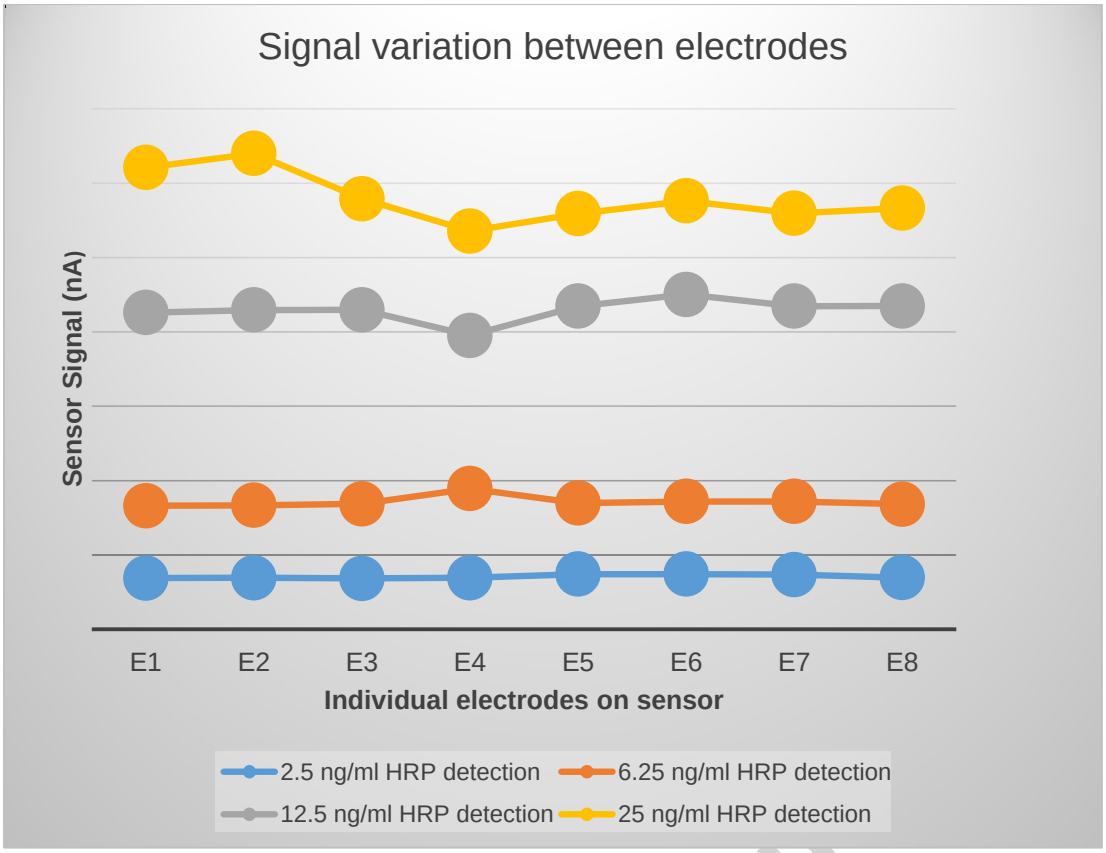

Figure 1: A) Comparison of HRP-TMB assays depending on incubation. Red columns represent results without incubation while dark blue columns show the results of incubated samples on individual electrodes of a sensor chip (n=3). B) Effect of different surface coatings (100% MUDA or 80% MUDA) on HRP detection. The results represent HRP binding responses on each individual electrodes (n=3). C) Overall results of HRP-TMB assays in the concentration range of 2.5-25 ng mL^{-1} on separate electrodes (n=3). D) Signal variation between individual electrodes of a sensor chip based on HRP concentration.

After the selection of most convenient conditions for HRP-TMB assays, HRP was successfully measured in the concentration range of 2.5-25 ng mL^{-1}. The results demonstrated the consistency of the sensor signals between the separate electrodes and also the chips. This is a vital achievement which verifies the workability and capability of the sensor to be developed for biological analysis. **Fig. 1**C displays the overall results obtained from different HRP concentrations on the individual electrodes. The variation between the electrodes were in acceptable range with small deviation on the data. Moreover, the sensor signal reached to the saturation after 12.5 ng mL^{-1} of HRP concentration. The standard error between the electrode signals was found to be very little in the case of low HRP concentration while it

was slightly higher for higher amounts of HRP. However, this did not cause any problem since the variation was proportional with the sensor signal (**Fig. 1**D).

3.2. *E. coli* detection assays

The SAM coated surface of the electrodes were checked using cyclic voltammetry. The characterization of five separate sensor chips was performed using K4[Fe(CN)6] / KCl to determine the quality and reliability of the sensor system. The same electrode of separate sensor chips produced similar CV scans with expected oxidation and reduction peaks (**Fig. 2**A). The individual electrodes of a certain sensor chip were also characterized to see the signal difference between the electrodes. The SAM coated individual electrodes produced nearly identical results (**Fig. S1**) and they demonstrated much narrower oxidation-reduction peaks due to denser surface than those of bare chip (**Fig. S2**). Furthermore, MUDA coated and EDC-NHS applied sensor surfaces were characterized using FT-IR where SAM formation and activation of the surface by EDC-NHS were confirmed (**Fig. S3**). Two different antibody concentrations (25 µg mL^{-1} and 50 µg mL^{-1}) were then tested to determine the optimal immobilization conditions for *E. coli* detection. For this, a fix concentration of the bacterium (3.5×10^6 cfu mL^{-1}) was tested. Although a good level of binding were obtained with 25 µg mL^{-1} of antibody, a clear increase on the sensor signal (~34.1 %) was observed while using 50 µg mL^{-1} concentration of the surface antibody (**Fig. 2**B). Therefore, higher concentration was used in the following steps of this research. Majority of the bacterial sensors reported in the literature have used much higher concentration of the surface antibody which increases the cost of the developed assays significantly (Masdor et al. 2016; Salam et al. 2013). A 150 µg mL^{-1} of anti-*E. coli* antibody was used for the specific detection of this bacterium in the concentration range of 10^4–10^7 cfu mL^{-1} by employing microelectrode array biosensor (Radke and Alocilja 2005).

A)

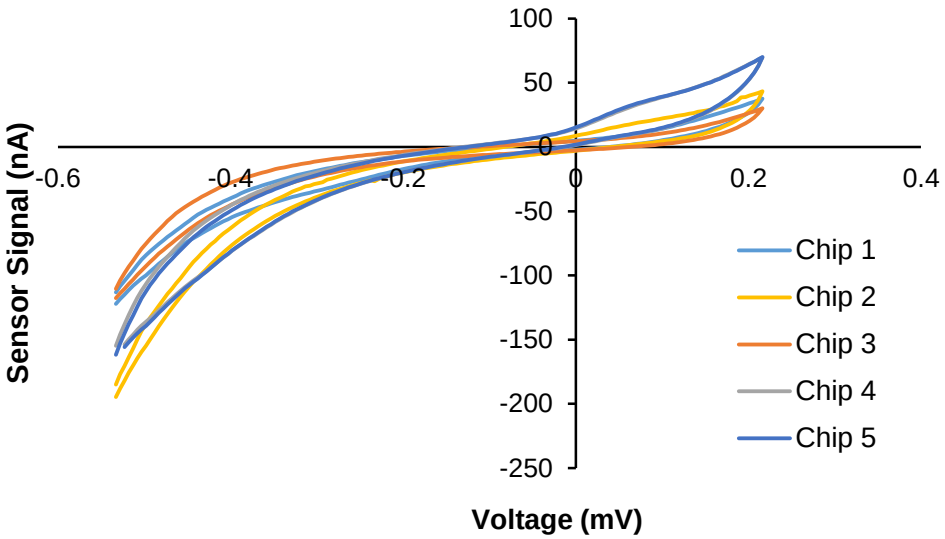

B)

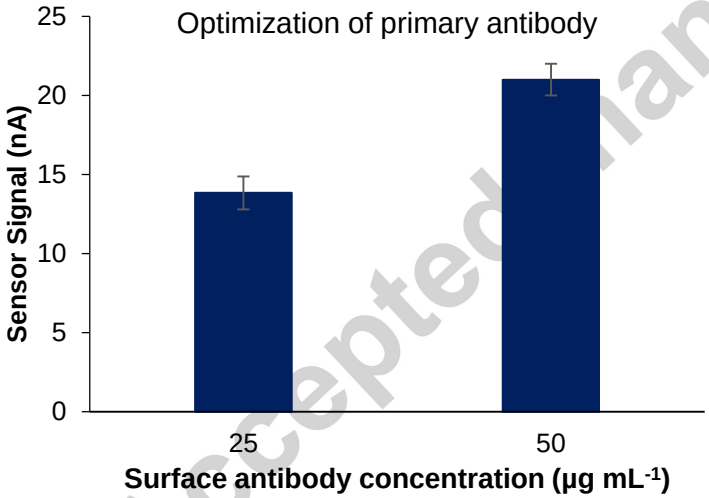

C)

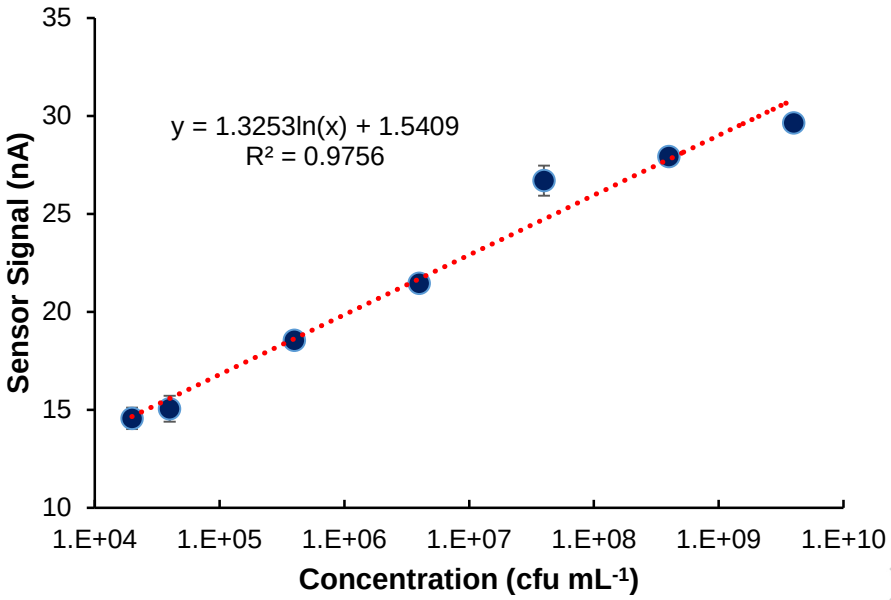

Figure 2: A) CV characterization of five separate sensor chips using the same electrode (electrode 2) to compare the difference between chips. B) Comparison of *E. coli* detection using two different surface antibody concentrations and optimization of antibody immobilization (n=3). C) Detection of *E.coli* in the concentration range of 1.99×10^{4}–3.98×10^{9} cfu mL^{-1} using standard sandwich assay (n=9).

3.2.1. Standard sandwich assay

E. coli samples purchased from SeraCare Life Sciences (Gaithersburg, USA) were prepared from the 1 mL of stock solution which contains 3.98×10^{9} cfu mL^{-1} bacteria. *E. coli* was investigated in the concentration range of 0.99×10^{4}-3.98×10^{9} cfu mL^{-1} using standard sandwich assay that provided a detection limit of 1.99×10^{4} cfu mL^{-1} (**Fig. 2**C). The overall data was subjected to the logarithmic regression analysis since it exhibited a straight-line relationship when graphed with the x values (bacteria concentration) on a log scale and the y values on a linear scale (sensor response). In this model, bacteria concentration is the independent variable whereas the sensor response is the dependent variable observed by the researcher (**Fig. 2**C). During the *E. coli* detection assays, each sample of the bacterium was injected to the surface for 8 minutes (25 µl min^{-1}) followed by HRP-conjugated detector antibody injection (8 min, 25 µl min^{-1}). Sandwich assays without nanomaterial applications generally cannot provide detection limits lower than 10^{3}–10^{4} cfu mL^{-1} for bacteria quantification (Masdor et al. 2017; Masdor et al. 2016; Radke and Alocilja 2005). Therefore,

gold nanoparticle enhanced sandwich assay approach was evaluated to increase the assay sensitivity for *E. coli* detection as the next step.

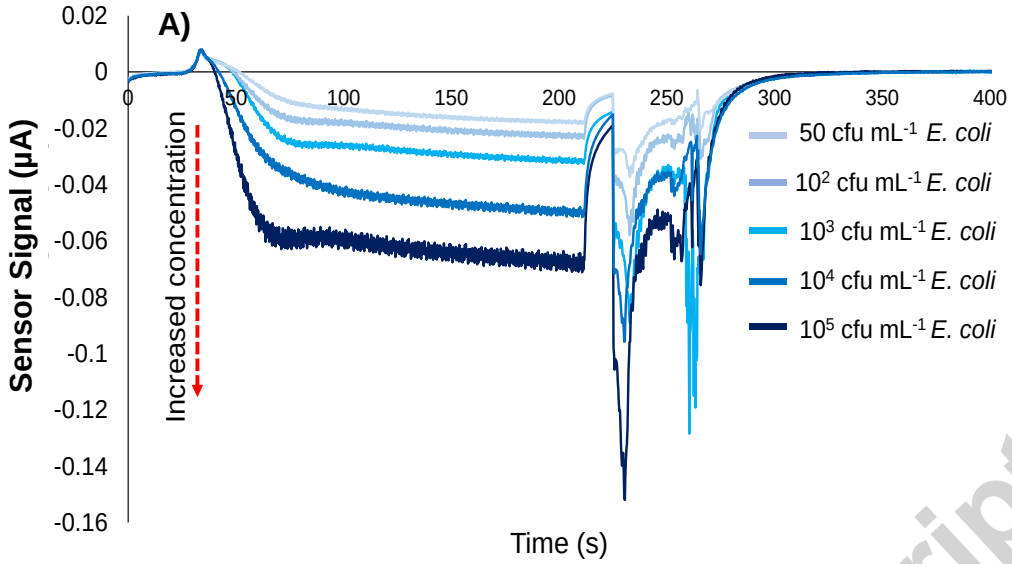

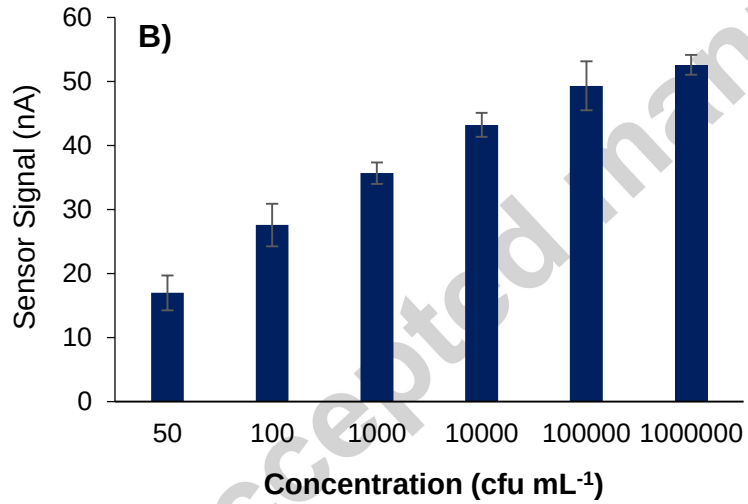

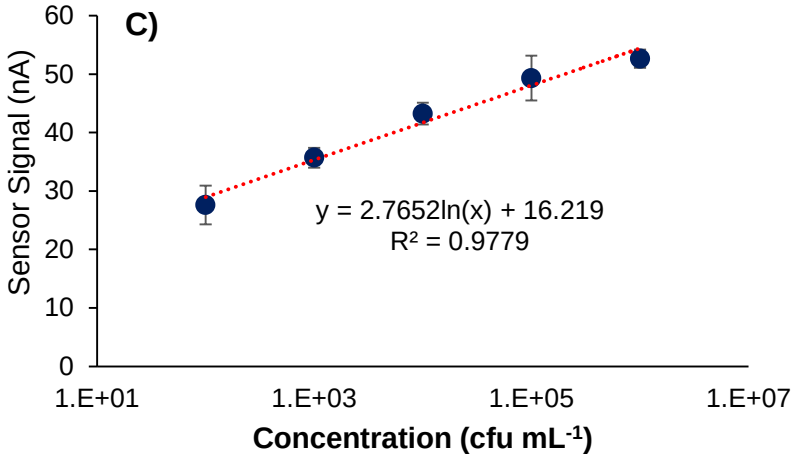

Figure 3: A) Concentration dependent real-time sensorgram of AuNP functionalized *E. coli* assay on a particular electrode. B) Detection of *E. coli* samples in PBS buffer in the concentration range of 50–10^6 cfu mL^{-1} using AuNP functionalized sensor assay. (C) Logarithmic regression analysis for overall assay results (n=9).

3.2.2. Signal amplification assays with gold nanomaterials

The utilization of AuNPs allowed to quantify *E. coli* down to 50 cfu mL^{-1}. The concentration dependent sensorgram displays a clear difference between the measured concentrations on the same electrode (**Fig. 3**A). The overall results of AuNP signal amplification assays were summarized in **Fig. 3**B. It is shown that MiSens biosensor is compatible to be employed for pathogenic bacteria detection with high sensitivity. When all data were subjected to the logarithmic regression analysis, a very good correlation with an R^2 value of 0.97 could be achieved (**Fig. 3**C). Batch-to-batch variation of AuNP preparation was also investigated prior to conduct the assays in water samples since it generally leads to a significant variation on the sensor results. For this, four different concentrations of *E. coli* (1.5×10^5, 1×10^6, 1.5×10^6 and 1.7×10^6 cfu mL^{-1}) were tested. After a careful analysis of the data, it was observed that the batch to batch variation of AuNP preparation did not lead to a major difference between the results (**Fig. 4**). A very recent research has reported the quantification of *E. coli* using gold nanoparticles based immunoassay by employing an electrochemical biosensor (Guner et al. 2017). This sensor relied on the Polypyrrole/AuNP/multi-walled carbon nanotubes/Chitosan hybrid bionanocomposite modified pencil graphite electrode (PGE). The monoclonal antibody was immobilized onto the surface and *E. coli* detection was achieved in the concentration range of 3×10^1 – 3×10^7 cfu mL^{-1} only in PBS buffer. The effect of batch to batch variation of AuNPs were also not reported (Guner et al. 2017). The currently developed

method has also shown superiority over the other methods in terms of sensitivity, easiness and rapidity. An impedance sensor developed for *E. coli* detection resulted in an LOD of 10^3 cfu mL^{-1} with an assay time of approximately a couple of hours (Li et al. 2014). Microfludic based biosensor for *E. coli* detection using antimicrobial peptide-labelled beads also resulted in an LOD of ~ 10^3 cfu mL^{-1} with a detection time of 30 min per sample (Yoo et al 2014) whereas our method achieved to quantify this bacterium down to 50 cfu mL^{-1} only in 8 minutes. The similar assay strategy using standard and AuNP-amplified sandwich assays were used for the detection of other bacteria by employing quartz crystal microbalance (QCM)- (Masdor et al. 2016) and surface plasmon resonance (SPR)-based (Masdor et al. 2017) sensors. However, the sensitivity of these sensors were lower, penetration depth was also a problem in case of using SPR technique.

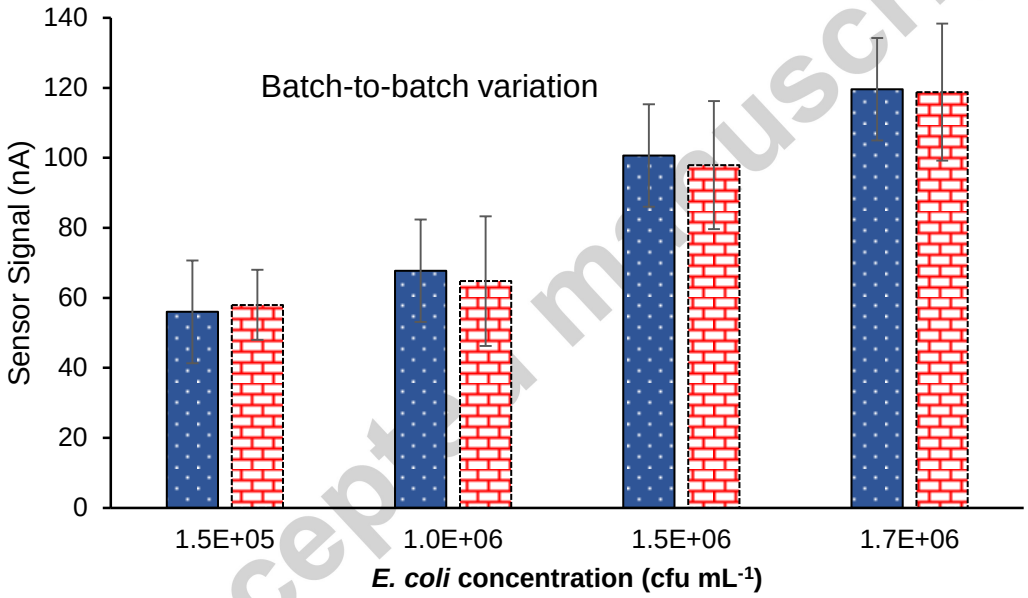

Figure 4: Effect of batch-to-batch variation of AuNP preparation on the sensor results (n=3). Blue columns demonstrate the results of batch 1 (AuNP functionalized detector antibody production 1) and red columns display the output of batch 2 (AuNP functionalized detector antibody production 2).

3.3. *E. coli* detection in water samples

To assess the potential application of MiSens biosensor for pathogenic bacteria detection in real samples, the developed sensor assay with AuNP functionalization was utilized for the

quantification of *E. coli* in water. A concentration range from 10 to 10^7cfu mL^{-1} was investigated and a detection limit of 50 cfu mL^{-1} was obtained with a correlation coefficient of 0.96 (**Fig. 5**A). The LOD was determined based on the experimental studies. The concentrations lower than 50 cfu mL^{-1} were also tested; however, the sensor signal was found to be similar to that of water. Each bacteria sample and AuNP-HRP labelled detector antibody were injected into the surface during 8 min injection (25 µl min^{-1}) subsequently. Later, the injection of the enzyme substrate (TMB/H_2O_2 solution) and simultaneous amperometric measurement against the applied potential (-0.1 V) resulted in a real-time amperometric signal that is proportional to the bound *E. coli* on the biochip surface.

Although a clear difference could be achieved between the investigated concentrations (**Fig. 5**B), 10 cfu mL^{-1} did not produced any signal. Moreover, when the results of real sample analysis were compared with those of samples in PBS buffer it can be concluded that MiSens biosensor has shown a significant compatibility with water and it does not require any special treatment or does not lead to a significant lose on the sensor signal. The same detection limit was successfully achieved both in PBS and water using gold nanomaterial's functionalization. 50 cfu mL^{-1} of *E. coli* produced 16.98 nA and 12.14 nA responses in PBS and water, respectively. Varshney et al (2007) reported a label free, microfluidics based impedance biosensor for the detection of *E. coli* in food samples. In this work, magnetic nanoparticle-antibody conjugates (MNAC) were prepared by conjugating streptavidin-coated magnetic nanoparticles with biotin-labeled polyclonal goat anti- *E. coli* antibodies and were used in the separation and concentration of target bacteria. The *E. coli* cells inoculated in a food sample were first captured by the MNAC, separated, and concentrated by applying a magnetic field, washed, and then suspended in mannitol solution and finally injected through the microfluidic flow cell for impedance measurement. This impedance biosensor was able to detect as low as 1.6×10^2 and 1.2×10^3 cells of *E. coli* O157:H7 cells present in pure culture and ground beef sample, respectively. The total detection time from sampling to measurement was 35 min (calculated after antibody immobilization). Although the required detection time is similar to the current work (32 min), our sensor achieved higher sensitivity with less complex assay procedure and the reuse of the same sensor surface is also possible for testing of different *E. coli* concentrations. TaqMan based PCR technique was used to quantify *E. coli* in water samples. The detection of bacterium was investigated in the range of 10^3- 10^7 cfu mL^{-1} that provided an LOD of 10^3 cfu per PCR tube. The assay required 5 h after overnight enrichment step (Frahm et al. 2003).

Multiplex real-time PCR assay based on immunomagnetic separation was used to detect other bacteria in food samples which resulted in a good sensitivity (LOD: 10 cfu g^{-1}). However, the investigation range was quite narrow (10^1–10^4 cfu mL^{-1}) and the assay time was still too long (8 h) (Ma et al. 2014).

A)

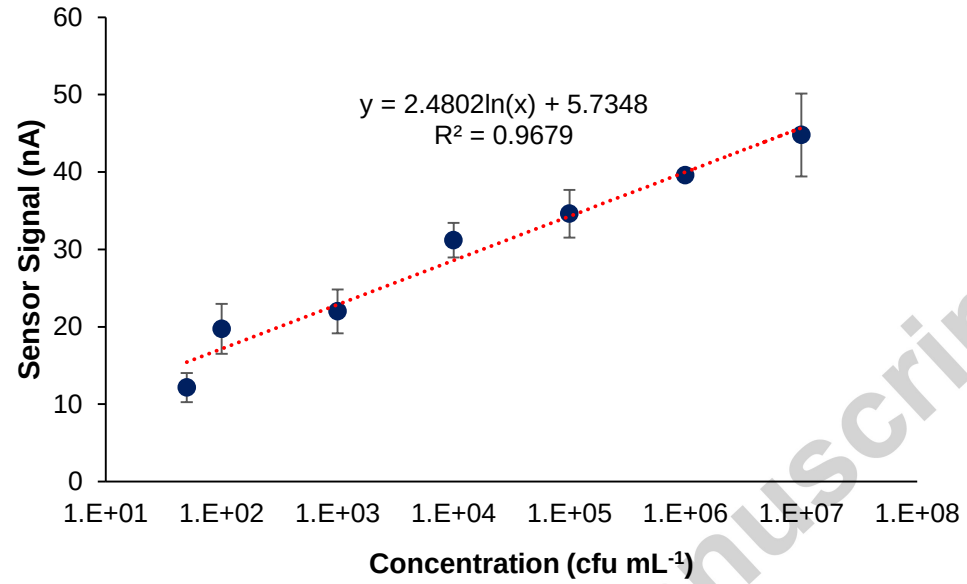

B)

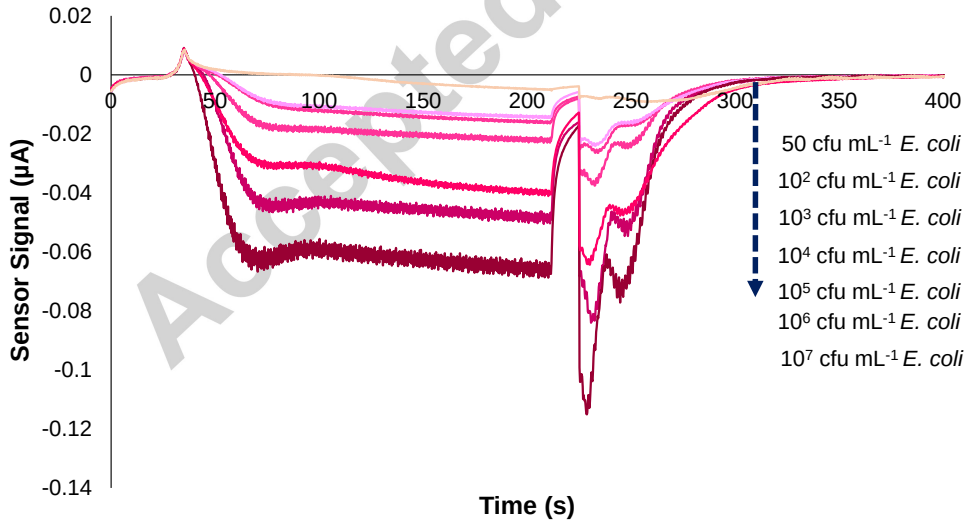

C)

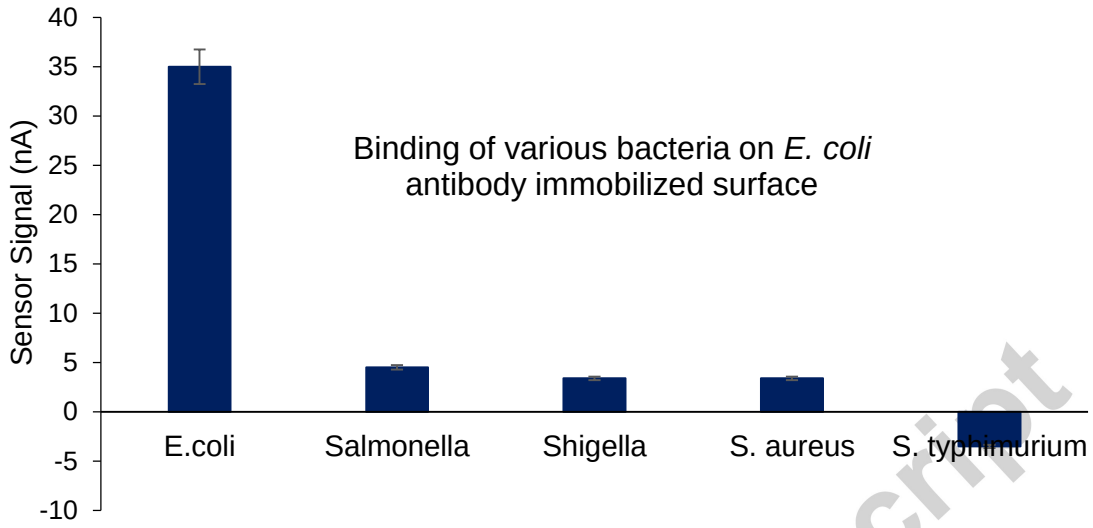

Figure 5: A) Determination of *E. coli* in water samples in the concentration range of 50–10^7cfu mL^{-1} with an R^2 value of 0.96. B) Real-time data of *E. coli* detection in water samples from 50 cfu mL^{-1} to 10^7 cfu mL^{-1}. C) Cross-reactivity investigations for *E. coli* specific sensor assay. All data is control subtracted (n=9).

3.4. Cross-reactivity studies for *E. coli*

To check the specificity of the assays for *E. coli*, the binding of non-specific bacteria on *E. coli* antibody immobilized surfaces was investigated. A 10^4 cfu mL^{-1} concentration of *Shigella, Salmonella* spp., *Salmonella typhimurium* and *Staphylococcus aureus* was injected into the sensor and the binding results were evaluated in addition to the specific binding of 10^4 cfu mL^{-1} *E. coli.* As it can be seen from **Fig. 5**C, a clear difference was observed between *E. coli* and non-specific bacteria binding on the surface which confirms the specificity of the developed sensor assays. Non-specific binding response of *Salmonella* was calculated as 12.8 %, followed by *Shigella* and *S. aureus* with 9.7%. *Salmonella typhimurium* did not bind to the sensor surface (0 %) and created negative sensor signal (-3.5 nA).

4. Conclusions

This work reports the successful design and manufacture of a novel microfluidic-based electrochemical biosensor for the sensitive, specific and rapid detection of a waterborne pathogen *E. coli*. A detection limit of 50 cfu mL^{-1} was achieved in water samples using the nanomaterial amplified immunosensor assay. The use of nanomaterial approach substantially improved the sensor results and increased the detection limit 398 fold when compared to standard sandwich assay. Furthermore, the sensor surface could be regenerated multiple times which significantly reduces the cost of the system. This comprehensive study demonstrates the great potential of our custom-designed biosensor to be employed in water and clinical sample analyses for pathogenic bacteria detection.

Acknowledgement

Z.A. thanks to TUBITAK-BIDEB for financial support of this project under 2221 program**.** We gratefully acknowledge Bioelectronic Devices and Systems Group from BILGEM-TUBITAK for their contribution to the fabrication of the biochip and the sensing platform. We also thank to Selcuk Kilic and Umut Berberoglu from Public Health Agency of Turkey for providing *Salmonella, Shigella* and *Staphylococcus* samples for cross-reactivity studies.

References

Abbaspour, A., Norouz-Sarvestani, F., Noori, A., Soltani, N., 2015. Biosens. Bioelectron. 68, 149-155.

Adkins, J.A., Boehle, K., Friend, C., Chamberlain, B., Bisha, B., Henry, C.S., 2017. Anal. Chem. 89(6), 3613-3621.

Ahmed, A., Rushworth, J.V., Hirst, N.A., Millner, P.A., 2014. Clin. Microbiol. Rev. 27(3), 631-646.

Altintas, Z., Kallempudi, S.S., Sezerman, U., Gurbuz, Y., 2012a. Sens. Actuators B Chem. 174, 187-194.

Altintas, Z., Uludag, Y., Gurbuz, Y., Tothill, I., 2012b. Anal. Chim. Acta 712, 138–144.

Altintas, Z., Uludag, Y., Gurbuz, Y., Tothill, I.E., 2011. Talanta 86, 377-383

Boehle, K.E., Gilliand, J., Wheeldon, C.R., Holder, A., Adkins, J.A., Geiss, B.J., Ryan, E.P., Henry, C.S., 2017. Angew. Chem. Int. Ed. 56(24), 6886-6890.

Borgohain, R., Baruah, S., 2017. IEEE Sens. J. 17(9), 2649-2653.

Chan, K.Y., Ye, W.W., Zhang, Y., Xiao, L.D., Leung, P.H.L.M., Li, Y., Yang, M., 2013. Biosens. Bioelectron. 41, 532-537.

Chen, J., Andler, S.M., Goddard, J.M., Nugen, S.R., Rotello, V.M., 2017. Chem. Soc. Rev. 46(5), 1272-1283.

Ciftci, G.Y., Senkuytu, E., Incir, S.E., Yuksel, F., Olcer, Z., Yildirim, T., Kilic, A., Uludag, Y., 2016. Biosens. Bioelectron. 80, 331-338.

Florentin, A., Lizon, J., Asensio, E., Forin, J., Rivier, A., 2016. Am J Infect Control. 44(9), 1061-1062.

Frahm, E., Obst, U., 2003. J. Microbiol. Methods. 52 (1), 123-131.

Golabi, M., Kuralay, F., Jager, E.W.H., Beni, V., Turner, A.P.F., 2017. Biosens. Bioelectron. 93, 87-93.

Guner, A., Cevik, E., Senel, M., Alpsoy, L., 2017. Food Chem. 229, 358-365.

Guo, Y., Wang, Y., Liu, S., Yu, J., Wang, H., Wang, Y., Huang, J., 2016. Biosens. Bioelectron. 75, 315-319.

Hancock, C.M., Rose, J.B., Callahan, M., 1998. J Am Water Works Assoc. 90(3), 58-61.

Huang, Y., Mason, A.J., 2013. Lab Chip 13(19), 3929-3934.

Lazcka, O., Del Campo, F.J., Munoz, F.X., 2007. Biosens. Bioelectron. 22(7), 1205-1217.

Lemarchand, K., Lebaron, P., 2003. FEMS Microbiol Lett 218(1), 203-209.

Li, Y., Afrasiabi, R., Fathi, F., Wang, N., Xiang, C., Love, R., She, Z., Kraatz, H.B., 2014. Biosens. Bioelectron. 58, 193-199.

Ma, K., Deng, Y., Bai, Y., Xu, D., Chen, E., Wu, H., Li, B., Gao, L., 2014. Food Control 42, 87-93.

Masdor, N.A., Altintas, Z., Tothill, I.E., 2017. Chemosensors 2017, 5(2), 16, 1-15.

Masdor, N.A., Altintas, Z., Tothill, I.E., 2016. Biosens. Bioelectron. 78, 328-336.

Nataro, J.P., Kaper, J.B., 1998. Clin. Microbiol. Rev. 11(1), 142-201.

Olcer, Z., Esen, E., Muhammad, T., Ersoy, A., Budak, S., Uludag, Y., 2014. Biosens. Bioelectron. 62, 163-169.

Pawula, M., Altintas, Z., Tothill, I.E., 2016. Talanta 146, 823-830.

Radke, S.A., Alocilja, E.C., 2005. Biosens. Bioelectron. 20(8), 1662-1667.

Rasooly, A., Herold, K.E., 2006. J. AOAC Int. 89(3), 873-883.

Rasooly, A., Sergeev, N., Herold, K.E., 2007. Minerva Biotecnol 19(3), 105-116.

Salam, F., Uludag, Y., Tothill, I.E., 2013. Talanta 115, 761-767.

Struss, A., Pasini, P., Ensor, C.M., Raut, N., Daunert, S., 2010. Anal. Chem. 82(11), 4457-4463.

Uludag, Y., Esen, E., Kokturk, G., Ozer, H., Muhammad, T., Olcer, Z., Basegmez, H.I.O., Simsek, S., Barut, S., Gok, M.Y., Akgun, M., Altintas, Z., 2016a. Talanta 160, 381-388.

Uludag, Y., Narter, F., Saglam, E., Kokturk, G., Gok, M., Akgun, M., Barut, S., Budak, S., 2016b. Anal. Bioanal. Chem. 408(27), 7775-7783.

Vaisocherova-Lisalova, H., Visova, I., Ermini, M.L., Springer, T., Song, X.C., Mrazek, J., Lamacova, J., Lynn, N.S., Sedivak, P., Homola, J., 2016. Biosens. Bioelectron. 80, 84-90.

Varshney, M., Li, Y.B., Srinivasan, B., Tung, S., 2007. Sens. Actuators B Chem. 128(1), 99-107.

Velusamy, V., Arshak, K., Korostynska, O., Oliwa, K., Adley, C., 2010. Biotechnol. Adv. 28(2), 232-254.

Xu, M., Wang, R., Li, Y., 2016. Analyst. 141, 5441-5449.
Yang, Z.Q., Zhang, Y., Itoh, T., Maeda, R., 2014. Lab Chip 14(24), 4604-4608.

Yoo, J.H., Woo, D.H., Chang, M., Chun, M.-S., 2014. Sens. Actuators B Chem. 191, 211-218.

Zhang, X., Shen, J., Ma, H., Jiang, Y., Huang, C., Han, E., Yao, B., He, Y., 2016. Biosens. Bioelectron. 80, 666-673.

Highlights

- A novel custom-designed biosensor for pathogen detection was manufactured.
- A real-time electrochemical sensing platform with continuous microfluidic flow was demonstrated.
- Sensitive *E. coli* quantification was achieved in water samples with 50 cfu mL^{-1} LOD.
- The fully automated sensor can play a major role for the diagnosis of waterborne pathogens